# Optimization of helix angle for helical gear system[†]

## Ju Seok Kang[1] and Yeon-Sun Choi[2,*]

[1]*Dept. of Rolling Stock Mechanical Engineering, Korea National Railroad College,*
*374-18, Woram-dong, Uiwang-si, Kyunggi-do, 437-763, Korea*
[2]*School of Mechanical Engineering, Sungkyunkwan University,*
*300 Chunchun-dong, Jangan-gu, Suwon, Kyunggi-do, 440-746, Korea*

---

## Abstract

A method is presented to optimize the helix angle of a helical gear from the viewpoint of the transmission error, which is the deflection of the teeth due to the transmitted load. The deflection of the gear teeth is calculated by using the bending and shear influence function, which is formulated from the common formula for deflection obtained from FEM, and the contact influence function based on Hertzian contact theory. Tooth contact analysis is performed to calculate the contact lines of the helical gear, where the deflection of the tooth is measured. A numerical example is presented to explain a method to optimize the helix angle of a helical gear system. The relation between the contact ratio and transmission error is investigated through calculations of the variation in the transmission error with the helix angle.

*Keywords*: Helix angle; Helical gear; Transmission error; Influence function; Contact ratio

---

## 1. Introduction

In the design of power transmission systems, the prediction and control of gear vibration is essential because gears are one of the major vibro-acoustic sources. The load transmitted by a gear pair causes deflections of the teeth of the gear pair. As the contact position on the meshing gear teeth varies with the rotational angle, the tooth stiffness is also varied with the rotational angle. This resultant varied stiffness leads to variations in the transmission error, which is the major factor contributing to the dynamic sources of noise and vibration of a gear pair.

Dynamic measurements have verified that the mesh stiffness of a helical gear is roughly proportional to the sum of the lengths of the contact lines of all the tooth pairs in contact. The sum of the lengths of the contact lines has been used as an alternative to the transmission error, which is difficult to obtain for

a helical gear due to the complex contact geometry. However, the sum of the lengths of the contact lines can provide only an overall estimate of the transmission error and is not accurately coincident with the transmission error. Moreover, since the helix angle must be selected at an early design stage for a helical gear system, accurate calculations of the transmission error must be performed in order to obtain a suitable helix angle that optimizes the transmission error.

Numerical solutions to obtain the transmission error for a helical gear system have been presented by several authors [1-4]. Chen et al. [1] performed tooth contact analysis to determine the transmission error of a helical gear with a modified gear tooth profile. Ajmi et al. [2] showed that the modeling of the gear body flexibility is important to obtain the tooth load deflection for wide-face gears. Recently, several approaches have been proposed to obtain a solution for tooth deflection using FEM as an efficient tool [5-10]. An "Express model" was presented to reduce the computation times for FEM [5]. Anderson et al. [6] presented a method to determine the dynamic transmission error in a helical gear set by calculating the in-

---

stantaneous angular positions of contact by solving the dynamic equations for the gear system. General solutions for the transmission errors of helical gears based on the geometric parameters have been derived by solving for the deflection of a standard rack [11, 12]. However, in spite of such numerous approaches for calculating the transmission error of a helical gear, analysis of the influence of the helix angle on a helical gear from the viewpoint of the transmission error has not been reported.

In this paper, the actual positions of contact for a helical gear pair are calculated by tooth contact analysis to compute the contact lines on the teeth of the helical gear. The deflection due to the transmitted load is calculated on these contact lines so that the transmission error can be calculated with the gear rotational angles. FEM is used to find general solutions for the bending and shear deformation of the helical gear with the geometric parameters such as the pressure angle and width and height of the teeth. The bending and shear deformation of the tooth is determined by numerical integration of the influence function. The contact deformation of the teeth is calculated from Hertzian contact theory. The helix angle of a helical gear is the key factor that differentiates it from a spur gear in that the helix angle affords smoother contact, thereby reducing variations in the transmission error. Through a comparison between the helix angle and transmission error, the optimum helix angle that affords a constant transmission error is determined.

## 2. Equations for the transmission error

The transmitted load is distributed on the contact line of the gear tooth when two helical gears contact each other. The contact between the mating teeth is assumed to take place in the line of the tooth faces. The influence function can be used to calculate the deflection of the teeth due to the load distribution $p(\xi_L)$, as shown in Fig. 1. Considering a tooth pair in contact, the bending and shear deformations of each tooth, $\Delta_{b1}(x_L)$ and $\Delta_{b2}(x_L)$, along the contact line $L$ can be written as

$$\Delta_{b1}(x_L) = \int_L K_{b1}(x_L, \xi_L) p(\xi_L) d\xi_L \qquad (1)$$

$$\Delta_{b2}(x_L) = \int_L K_{b2}(x_L, \xi_L) p(\xi_L) d\xi_L \qquad (2)$$

where $K_{b1}(x_L, \xi_L)$ and $K_{b2}(x_L, \xi_L)$ are the influ-
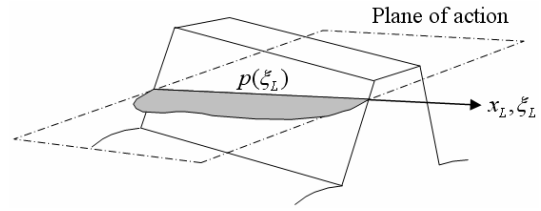


Fig. 1. Load distribution on the contact line of a gear.

ence functions due to the bending and shear deformations of each tooth in contact. These bending and shear influence functions represent the deflection at $x_L$ along the contact line $L$, where the load is applied at $\xi_L$. The cumulative deflection of both teeth in contact together is written as

$$\Delta_b(x_L) = \Delta_{b1}(x_L) + \Delta_{b2}(x_L)$$
$$= \int_L K_{b1}(x_L, \xi_L) p(\xi_L) d\xi_L + \int_L K_{b2}(x_L, \xi_L) p(\xi_L) d\xi_L \qquad (3)$$

If we set a combined influence function, $K_b(x_L) = K_{b1}(x_L, \xi_L) + K_{b2}(x_L, \xi_L)$, then the bending and shear deformation can be written as

$$\Delta_b(x_L) = \int_L K_b(x_L, \xi_L) p(\xi_L) d\xi_L \qquad (4)$$

Similarly, the deflection due to the contact loads is defined with the influence function for the contact deformation between the teeth in contact multiplied by the load distributions as

$$\Delta_c(x_L) = \int_L K_c(x_L, \xi_L) p(\xi_L) d\xi_L \qquad (5)$$

The influence function of the contact deformation $K_c(x_L, \xi_L)$ includes the deformation of each tooth in contact.

Thus, the total deflection from the combination of the bending and shear influence functions and the contact influence function can be summarized as

$$\Delta(x_L) = \Delta_b(x_L) + \Delta_c(x_L)$$
$$= \int_L K_b(x_L, \xi_L) p(\xi_L) d\xi_L \qquad (6)$$
$$+ \int_L K_c(x_L, \xi_L) p(\xi_L) d\xi_L$$

Since the teeth are in perfect contact along the full length of the contact line, the total deflection under

the load will be constant along the line of contact as

$$\Delta = \int_L K_b(x_L, \xi_L) p(\xi_L) d\xi_L + \int_L K_c(x_L, \xi_L) p(\xi_L) d\xi_L \quad (7)$$

Thus, we can define the transmission error of a tooth in contact as Eq. (7).

The transmitted load $F$ between the teeth in contact is equal to the sum of the load distribution on the contact line as

$$F = \int_L p(\xi_L) d\xi_L \quad (8)$$

Therefore, the transmission error of a helical gear pair can be obtained by solving Eqs. (7) and (8) simultaneously.

## 3. Tooth contact analysis

In order to find the transmission error in Eq. (7), we must first determine the contact line, where the influence functions are defined. For a helical gear, which has oblique contact lines on the tooth face due to the helix angle, tooth contact analysis must be performed. The contact line for a helical gear pair can be determined from the kinematic compatibility between the numerically generated surfaces of the teeth in contact.

To obtain the contact line between mating helical gears, the tooth face must be represented with an analytical surface formula. A screw involute surface can be generated by the screw motion of a straight line, as shown in Fig. 2 [13, 14]. The tooth flank of a left-hand helical gear and the unit normal to the surface shown in Fig. 2 are represented as follows.
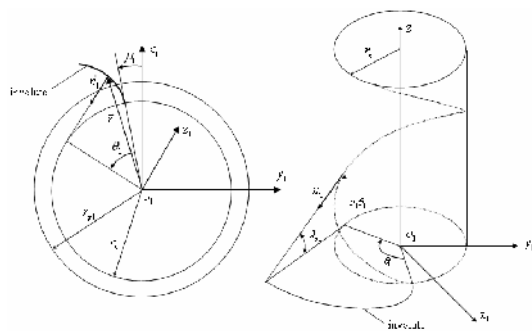


Fig. 2. Cross-section of a left-hand helical gear.

$$\vec{r}_1(u_1, \theta_1) = \begin{bmatrix} r_{b1} \cos(\theta_1 + \mu_1) + u_1 \sin(\theta_1 + \mu_1) \\ -r_{b1} \sin(\theta_1 + \mu_1) + u_1 \cos(\theta_1 + \mu_1) \\ -u_1 \sin \lambda_{b1} + p_1 \theta_1 \end{bmatrix} \quad (9)$$

$$\vec{n}_1(\theta_1) = \begin{bmatrix} -\sin \lambda_{b1} \sin(\theta_1 + \mu_1) \\ -\sin \lambda_{b1} \cos(\theta_1 + \mu_1) \\ \cos \lambda_{b1} \end{bmatrix} \quad (10)$$

The corresponding tooth surface of a right-hand gear and the unit normal to the surface are represented similarly as follows.

$$\vec{r}_2(u_2, \theta_2) = \begin{bmatrix} r_{b2} \cos(\theta_2 - \mu_2) + u_2 \sin(\theta_2 - \mu_2) \\ -r_{b2} \sin(\theta_2 - \mu_2) + u_2 \cos(\theta_2 - \mu_2) \\ u_2 \sin \lambda_{b2} - p_2 \theta_2 \end{bmatrix} \quad (11)$$

$$\vec{n}_2(u_2, \theta_2) = \begin{bmatrix} \sin \lambda_{b2} \sin(\theta_2 - \mu_2) \\ \sin \lambda_{b2} \cos(\theta_2 - \mu_2) \\ -\cos \lambda_{b2} \end{bmatrix} \quad (12)$$

where $r_{bi}$ $(i = 1, 2)$ and $r_{pi}$ $(i = 1, 2)$ are the radii of base circle and pitch circle, respectively; $\mu_i$ $(i = 1, 2)$, the start angles of the helicoids surfaces; $p_i$ $(i = 1, 2)$, the pitches at the base circles; and $\lambda_{bi}$ $(i = 1, 2)$, the lead angles of the helicoid surfaces at the base circles. $\theta_i (i = 1, 2)$ are the surface parameters defined as shown in Fig. 2. In this paper, the new parameters $z_i (i = 1, 2)$ are used instead of the surface parameters $u_i (i = 1, 2)$ to represent the height of a gear tooth effectively in Eqs. (9) and (11) by using the relation

$$u_i = \frac{p_i \theta_i \mp z_i}{\tan \lambda_{bi}}, \quad i = 1, 2 \quad (13)$$

With the given input design parameters such as the radii of the base circles $r_{bi}$ $(i = 1, 2)$, numbers of teeth $Z_i$ $(i = 1, 2)$, pressure angles $\alpha_{ni}(i = 1, 2)$, normal modules $m_i(i = 1, 2)$, and helix angles at the pitch circles $\beta_i(i = 1, 2)$, the parameters in Eqs. (9)~(12) are defined as follows.

$$r_{pi} = \frac{Z_i m_i}{2 \cos \beta_i} \quad i = 1, 2 \quad (14)$$

$$\lambda_{bi} = \tan^{-1}\left(\frac{r_{pi}}{\tan \beta_i r_{bi}}\right), \quad i = 1, 2 \quad (15)$$

$$\mu_i = \frac{\pi}{2 Z_i} \mp [\tan \alpha_{ti} - \alpha_{ti}], \quad i = 1, 2 \quad (16)$$

$$p_i = r_{bi} \tan \lambda_{bi}, \quad i = 1, 2 \quad (17)$$
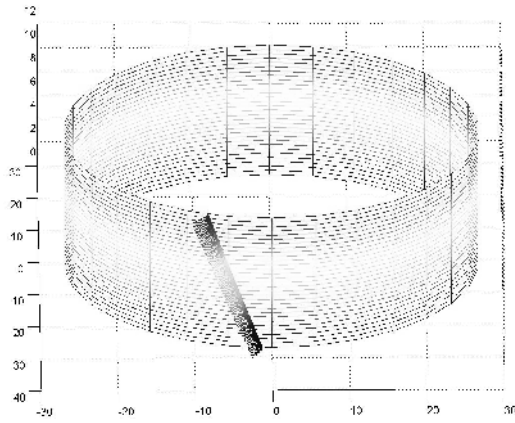
Fig. 3. Generated surface of a left-hand helical gear.
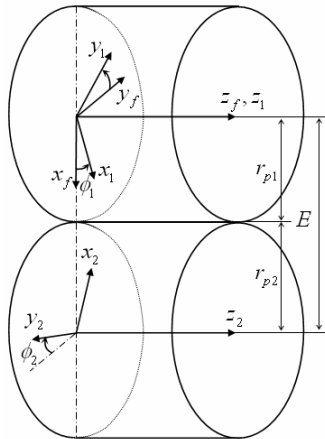


Fig. 4. Coordinate systems for a helical gear pair.

An example of the helicoid surface of a left-hand helical gear obtained with the above equations is shown in Fig. 3.
Coordinate systems that are rigidly connected to the gears can be transformed to fixed coordinate systems as shown in Fig. 4 as

$$\vec{r}_f^{(1)} = \begin{bmatrix} \cos\phi_1 & -\sin\phi_1 & 0 \\ \sin\phi_1 & \cos\phi_1 & 0 \\ 0 & 0 & 1 \end{bmatrix} \vec{r}_1 \tag{18}$$

$$\vec{r}_f^{(2)} = \begin{bmatrix} -\cos\phi_2 & -\sin\phi_2 & 0 \\ \sin\phi_2 & -\cos\phi_2 & 0 \\ 0 & 0 & 1 \end{bmatrix} \vec{r}_2 + \begin{bmatrix} E \\ 0 \\ 0 \end{bmatrix} \tag{19}$$

$$\vec{n}_f^{(1)} = \begin{bmatrix} \cos\phi_1 & -\sin\phi_1 & 0 \\ \sin\phi_1 & \cos\phi_1 & 0 \\ 0 & 0 & 1 \end{bmatrix} \vec{n}_1 \tag{20}$$

$$\vec{n}_f^{(2)} = \begin{bmatrix} -\cos\phi_2 & -\sin\phi_2 & 0 \\ \sin\phi_2 & -\cos\phi_2 & 0 \\ 0 & 0 & 1 \end{bmatrix} \vec{n}_2 \tag{21}$$

where $\phi_1$ and $\phi_2$ are the rotational angles of each gear in contact.

Using the surfaces defined in the fixed coordinate system described by Eqs. (18)-(21), the contact lines can be obtained by geometric compatibility. The conditions of continuous tangency of gear tooth surfaces can be represented as

$$\vec{r}_f^{(1)}(z_1,\theta_1,\phi_1) - \vec{r}_f^{(2)}(z_2,\theta_2,\phi_2) = 0 \tag{22}$$

$$\vec{n}_f^{(1)}(\theta_1,\phi_1) - \vec{n}_f^{(2)}(\theta_2,\phi_2) = 0 \tag{23}$$

Eqs. (22) and (23) yield only five independent equations since the auxiliary equation $\left|\vec{n}_f^{(1)}\right| = \left|\vec{n}_f^{(2)}\right| = 1$. Therefore, using Eqs. (22) and (23), the variables $z_1, \theta_1, z_2, \theta_2, \phi_2$ defined at the contact line can be obtained for arbitrary rotational angles $\phi_1$.
Generally, there are several teeth that are in contact simultaneously for a helical gear pair. The number of teeth in contact is the same as the number of sets of variables satisfying Eqs. (22) and (23). The sum of the lengths of the contact lines can be determined by summing the lengths of these contact lines.

## 4. Influence functions of deformation

After the contact lines of the teeth are obtained, the influence function in Eq. (3) must be defined and calculated on the contact lines. The influence function of bending and shear deformation is established from FEM analysis. In order to have a general solution for the transmission error with the geometric parameters, the common function of deflection is calculated by using approximate formulas.

In Eq. (7), the influence function for bending and shear deformation is defined along the contact line based on $x_L$ and $\xi_L$, where $x_L$ is the point of deflection measured due to a unit load at $\xi_L$. Here, 2-dimensional coordinates $(x,y)$ and $(\xi,\eta)$ are used to represent the influence function for arbitrary helical gears. The influence functions of bending and shear for each gear in contact, $K_{b1}(x,y,\xi,\eta)$ and $K_{b2}(x,y,\xi,\eta)$, which are the deformations at the point $(x,y)$ on the line of contact due to a unit force at the point $(\xi,\eta)$, can be generalized with the common formulas for the deflections of a tooth of height
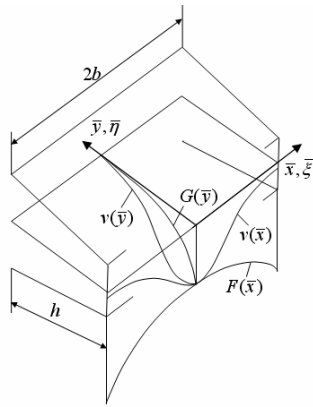
Fig. 5. Assumed influence function.



Fig. 6. A FEM model.

$h$ and width $2b$, as shown in Fig. 5. The bending and shear influence function is written with the common formulas for the deflections as

$$K_{bi}(x,y,\xi,\eta) = U \frac{v(\overline{r})}{\sqrt{F(\overline{x}-\overline{\xi})G(\overline{y}-\overline{\eta})}}$$

$$\sqrt{F(\overline{x})F(\overline{\overline{\xi}})G(\overline{y})G(\overline{\overline{\eta}})}, \quad i=1,2$$

(24)

where $\overline{r}^2 = (\overline{x}'-\overline{\overline{\xi}}')^2 + (\overline{y}-\overline{\eta})^2$. In order to represent the bending and shear influence function with the common formula for deflections, the nondimensional coordinates $(\overline{x},\overline{y},\overline{\xi},\overline{\eta})$, which are the coordinates $(x,y,\xi,\eta)$ divided by the height of the gear tooth $h$, are used in Eq. (24). $\lambda$ denotes the scale factor such that $\overline{x}' = \lambda\overline{x}$ and $\overline{\overline{\xi}}' = \lambda\overline{\overline{\xi}}$. U denotes the absolute value of the deflection at the center of the tip. $v(\overline{r})$ is the common deflection function in the circular direction; $F(\overline{x})$, the common deflection function in the direction of the width; and $G(\overline{y})$, the common deflection function in the direction of the height. These functions can be computed by FEM analysis with the parameters of the pressure angle, tooth height, and tooth width for a standard rack of gear teeth, as shown in Fig. 6. To calculate the bending and shear deformation simultaneously, solid elements with three translational coordinates are used for the FEM analysis.

Even for gears with the same pressure angle and module, there can be numerous different gear profiles, depending on the base circle. However, since the purpose of this study is to optimize the helix angle for a helical gear system, small variations in the gear profile are neglected in order to obtain a general solution with the parameters. The influence functions for gears with the same specific module and pressure
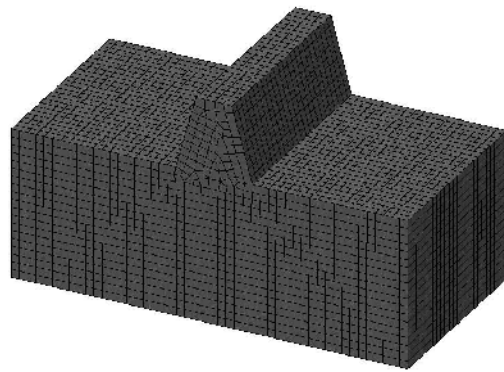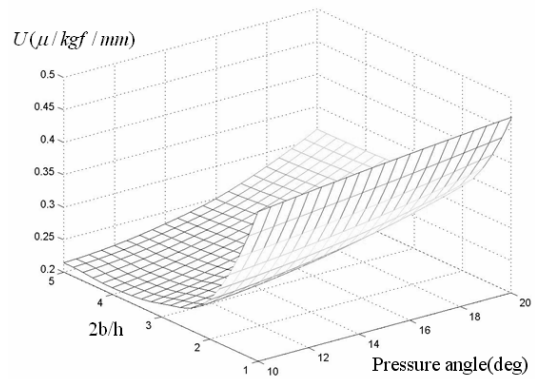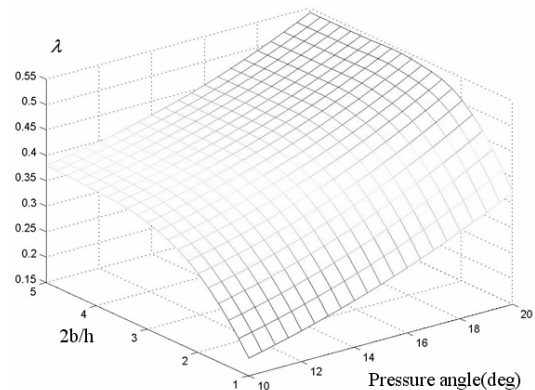


Fig. 7. Absolute deflection of origin.



Fig. 8. Scale factor $\lambda$.

angle are assumed to be the same as those of the representative standard rack, which is used for the FEM analysis.

From the FEM analysis, U in Eq. (24) is determined by the pressure angle and the value of $2b/h$, as shown in Fig. 7. Fig. 8 shows the scale factor $\lambda$ as a function of the pressure angle and the value of
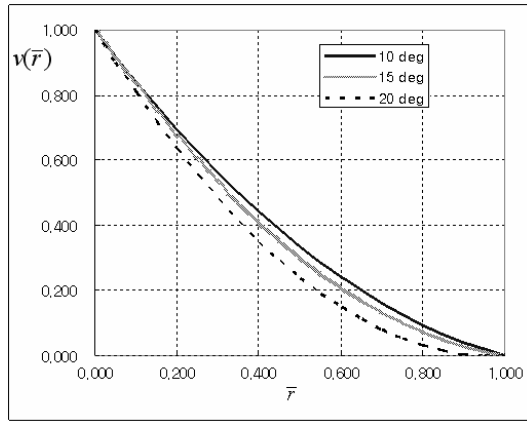
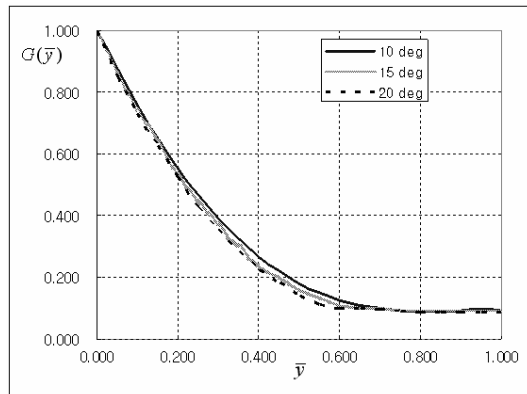Fig. 9. Common function of deflection in the direction of circulation.



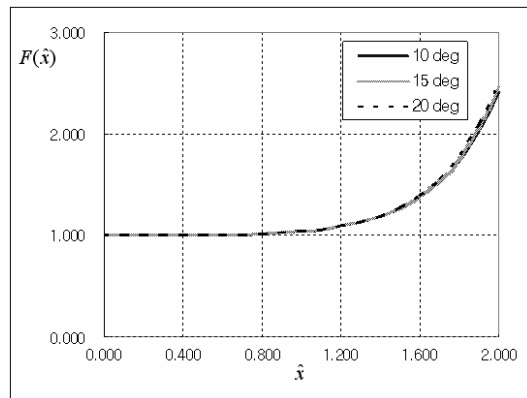Fig. 10. Common function of deflection in the height direction.



Fig. 11. Common function of deflection in the width direction.

$2b/h$. Figs. 9, 10, and 11 show the common deflection functions in the direction of circulation, tooth width, and tooth height, respectively, or $v(\overline{r})$, $F(\overline{x})$,
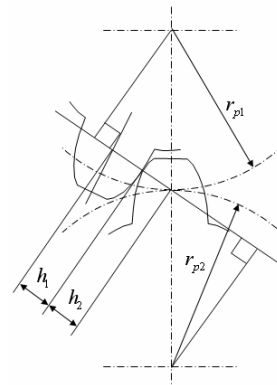


Fig. 12. Position of contact on the gears.

and $G(\overline{y})$. $v(\overline{r})$, $F(\overline{x})$, and $G(\overline{y})$ can be represented as functions of the pressure angle only. Consequently, the deflection due to bending and shear of a helical gear tooth can be calculated with these common functions by numerical interpolation with arbitrary values of the pressure angle, tooth height, and tooth width.

The influence function of contact deformation is calculated based on Hertzian contact theory. When contact problems in gears are discussed, in particular, Weber and Banaschek's equation is generally used to obtain the analytical solution [15]. The deformation of a tooth pair in contact due to the Hertzian contact pressure, as shown in Fig. 12, is calculated by using the formula

$$
u_c = \frac{2P}{\pi L}\left[\frac{1-\nu_1^2}{E_1}(\ln\frac{2h_1}{b} - \frac{\nu_1}{2(1-\nu_1)}\right.
$$
$$
\left. + \frac{1-\nu_2^2}{E_2}(\ln\frac{2h_2}{b} - \frac{\nu_2}{2(1-\nu_2)}\right]
\tag{25}
$$

where b is the extension of the load, which is calculated as

$$
b = \sqrt{\frac{4P}{\pi L}\left[\frac{1-\nu_1^2}{E_1} + \frac{1-\nu_2^2}{E_2}\right]\frac{\rho_1\rho_2}{\rho_1+\rho_2}}
\tag{26}
$$

where $E_i(i=1,2)$ and $\nu_i(i=1,2)$ are Young's moduli and Poisson ratios for each gear in contact, and $\rho_i(i=1,2)$ are taken as the radii of curvature at the pitch point. $h_1$ and $h_2$ are the lengths on the line of application from the contact point to the center of the teeth, as shown in Fig. 12. Under the assumption that the influence function of contact deformation

only has an effect on the point at which the load is applied, the contact deformation can be written as

$$\int_L K_c(x_L, \xi_L) p(\xi_L) d\xi_L = K_c(x_L) P(x_L) \tag{27}$$

where $K_c(x_L)$ is determined using Eq. (25).

The coordinates of the contact line obtained by the tooth contact analysis in the previous section must be transformed to the coordinates on the gear center plane, where the influence function is defined. As shown in Fig. 13, the contact point of the gear tooth surface, $\vec{r}_i(i=1,2)$, is transformed by appropriate transformation to the coordinates $(x, y)$ on the gear center plane. Therefore, the deflection due to the transmitted load can be computed on the contact line. A flow chart of the computational procedure used to calculate the transmission error numerically is shown in Fig. 14.
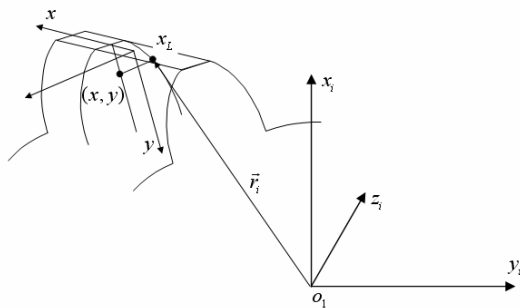


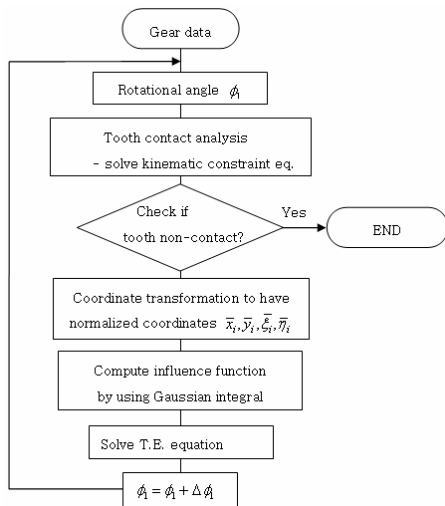Fig. 13. Contact point projected on the gear center plane.



Fig. 14. Flow chart for numerical analysis.

# 5. Results and discussions

In this paper, a gear set with the specifications shown in Table 1 has been analyzed. The calculated contact line on a tooth of a left-hand helical gear is shown in Fig. 15. The tooth surfaces of the mating helical gears contact each other along straight lines, as shown in Fig. 15. The number of these contact lines can be calculated by using the rotational angle of the gear. Fig. 16 shows the number of contact lines with various rotational angles. The number of contact lines in Fig. 16 varies in the range between three and four. Thus, the calculated contact ratio is 3.35, which

Table 1. Specification of gear pair.

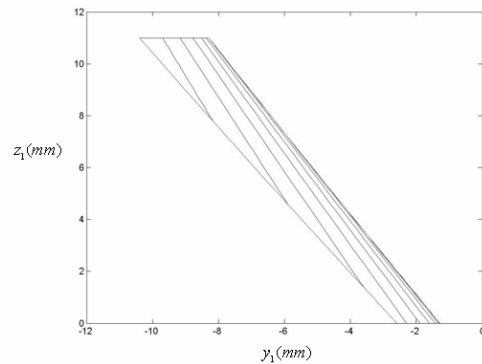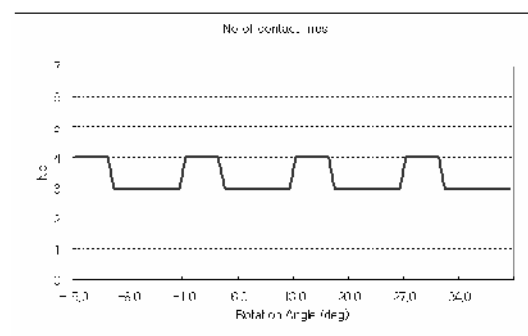| Parameter | Gear 1 | Gear 2 |
|---|---|---|
| No of tooth $Z_i$ | 27 | 30 |
| Normal module $m_i$ | 1.75 | 1.75 |
| Base radius(mm) $r_{bi}$ | 26.83 | 29.82 |
| Helix angle(deg) $\beta_i$ | 33 | 33 |
| Pressure angle(deg) $\alpha_{ni}$ | 15 | 15 |
| Tooth height(mm) $h$ | 3.28 | 3.31 |
| Tooth width(mm) $b$ | 13.12 | 13.12 |



Fig. 15. Contact lines on a tooth.
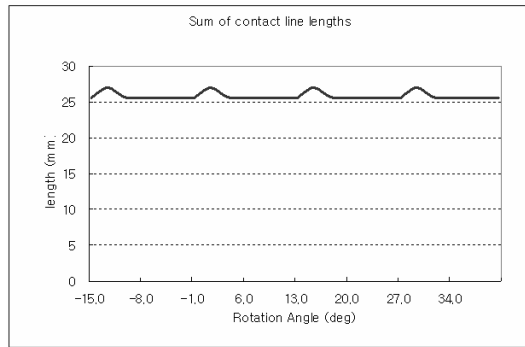


Fig. 16. Number of contact lines.

Fig. 17. Total length of contact lines.



Fig. 18. Estimated transmission error.



Fig. 19. Number of contact lines vs. helix angles.



Fig. 20. Lengths of contact lines vs. helix angles.
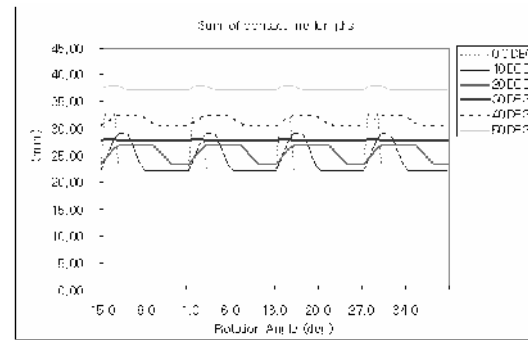


Fig. 21. Transmission errors vs. helix angles.

means that three teeth are in contact for 65% of the time and four teeth for the remaining 35%.

It is known that the mesh stiffness of a helical gear is roughly proportional to the sum of the lengths of the contact lines of the gears in contact. Generally, the sum of the lengths of the contact lines can be used as an alternative to the transmission error, which is difficult to obtain for helical gear. The sum of the lengths of the contact lines for the helical gear pair is shown in Fig 17. When three teeth are in contact, the sum of contact line lengths is 25.56 mm; when four teeth are in contact, it is 27.04 mm.

Fig. 18 shows the results of the transmission error for the helical gear pair described in Table 1 for a transmitted torque of 15 Nm. As shown in Fig. 18, the transmission error tends to be in inverse proportion to the sum of the contact line lengths; the transmission error varies between 1.19 and 1.13 µm.

The contact ratio for a helical gear pair increases with the helix angle, which generates the screwed surface of the tooth face. Here, the contact ratio, the sum of contact line lengths, and the transmission error for the pair are compared for various helix angles. Fig. 19 shows the number of teeth in contact for the
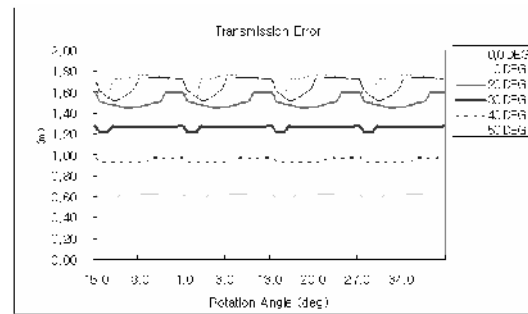
helical gear in Table 1 for helix angles of 0°, 10°, 20°, 30°, 40°, and 50°. The case of 0° is same as a spur gear. The number of teeth in contact increases with the helix angle as expected, as shown in Fig. 19.

Fig. 20 compares the sums of the lengths of the contact lines for various helix angles. When the helix angle is 0°, the change in the value of the sum of the contact line lengths reaches a maximum. However, when the helix angle is 30°, the sum of the contact line lengths is almost constant. The transmission errors are compared in Fig. 21. The magnitude of the transmission error decreases with an increase in the

helix angle, contrary to the relation with the sum of the contact line lengths. The variation in the transmission error also decreases with an increase in the helix angle.

The sum of the contact line lengths and the transmission error due to a change in the helix angle are investigated in detail. There would be no dynamic excitation from a helical gear pair without a corresponding variation in the transmission error in association with the rotational angle of the gear. Therefore, the variation in the sum of the contact line lengths and transmission error, which are the ratios of the maximum values to minimum values, are compared in Fig. 22. In Fig. 22, the overall trend in the variation of the sum of contact line lengths due to the helix angle is similar to that of the transmission error except at the minimum value. The variation in the sum of the contact line lengths is a minimum value when the helix angle is 30°; however, the variation in the transmission error has minima at helix angles of both 25° and 46°.

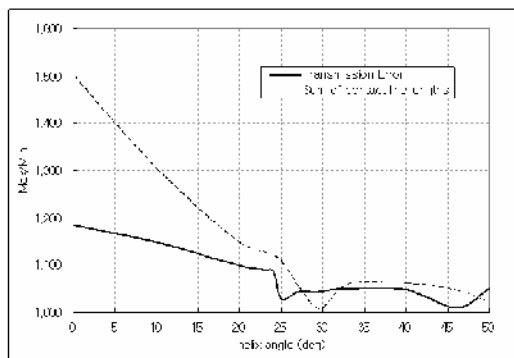Thus, from the viewpoint of the transmission error,



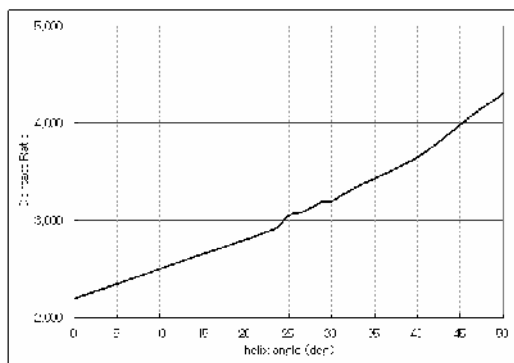Fig. 22. Transmission errors and contact line lengths vs. helix angles.



Fig. 23. Contact ratios vs. helix angles.

the helix angle should be either 25° or 46°; but 25° is preferred because extremely large helix angles such as 46° are difficult to manufacture. Fig. 23 shows the variation in the contact ratio with the helix angle. It is seen that the contact ratios have integer values of 3 and 4 when helix angles are around 25° and 46°, respectively. The helix angle at which the contact ratio is integral is coincident with the helix angle at which minimum variation in the transmission error occurs. In a helical gear system, the variation in the transmission error can be minimized when the contact ratio has an integer value. Therefore, the contact ratio provides more precise information than the sum of contact line lengths to determine the optimum helix angle for minimum variation in the transmission error.

## 6. Conclusions

A method to optimize the helix angle of a helical gear system by minimizing the variation in the transmission error with the gear rotational angle has been proposed. To calculate the transmission error, the influence function of tooth deflection was represented in a general form based on the design parameters of helical gears; this is useful in investigating helix angle effects. The contact line at which the influence function is defined was calculated based on the condition of kinematic compatibility between the mating tooth surfaces, which were generated by using numerical parameters.

In the numerical example, there exists a specific helix angle that minimizes the variation in the transmission error, which represents a dynamic excitation source for the gear system. This optimized helix angle is coincident with the helix angle at which the contact ratio has an integer value. The variation in the sum of contact line lengths due to the helix angle shows a trend similar to that of the transmission error, except for the minimum value. The contact ratio provides more precise information than the sum of contact line lengths for determining the optimum helix angle for minimizing the variation in the transmission error.

The optimized helix angle obtained in the numerical example is in the range of helix angles widely used in practice. Although the helix angle is one of the basic design parameters that must be determined at an early design stage, few such analytical methods have been proposed. The proposed approach enables the design of helical gears with minimized variations in the transmission error due to which the vibration

sources in rotary dynamic systems can be reduced.

## References

[1] Y. C. Chen and C. B. Tsay, "Contact ratios and transmission errors of a helical gear set with involute-teeth pinion and modified circular arc teeth gear," JSME International Journal, Series C,. 44 (3) 2001) 867-874.

[2] M. Ajmi and P. Velex, "A model for simulating the quasi-static and dynamic behaviour of solid wide-faced spur and helical gears," Mechanism and Machine Theory, 40 (2005) 173-190.

[3] M. Umeyama, M. Kato and K. Inoue, "Effects of gear dimensions and tooth surface modifications on the loaded transmission error of a helical gear pair," ASME J. of Mech. Design, 120 (1999) 119-125.

[4] P. Velex and V. Cahouet, "Experimental and numerical investigations on the influence of tooth friction in spur and helical gear dynamics," ASME J. of Mech. Design, 122 (2000) 515-522.

[5] R. Guilbault, C. Gosselin and L. Cloutirer, "Express model for load sharing and stress analysis in helical gears," ASME J. of Mech. Design, 127 (2005) 1161-1172.

[6] A. Andersson and L. Vedmar, "Dynamic model to determine vibrations in involute helical gears," J. of Sound and Vibration, 260 (2003) 195-212.

[7] Y. Zhang and Z. Fang, "Analysis of tooth contact and load distribution of helical gears with crossed axes," Mechanism and Machine Theory, 34 (1999) 41-57.

[8] J. Brauer, "A general finite element model of involute gears," Finite Elements in Analysis and Design, 40 (2004) 1857-1872

[9] F. L. Litvin, I. Gonzalez-Perez, A. Fuentes, D. Vecchiato, B. D. Hansen and D. Binney, "Design, generation and stress analysis of faced-gear drive with helical pinion," Comput. Methods Appl. Mech. Engrg. 194 (2005) 3870-3901.

[10] J. Hedlund and A. Lehtovaara, "Modeling of helical gear contact with tooth deflection," Tribology International, 40 (2007) Issue 4 613-619.

[11] K. Umezawa, T. Suzuki and T. Sato, "Vibration of power transmission helical gears (Approximate equation of tooth stiffness)," Bulletin of JSME, 29 (1986) 1605-1611.

[12] C. I. Park and D. S. Kim, "Transmission error analysis of helical gears for the elevator," Trans. of the KSME A, 26 (12) (2002) 2695-2702.

[13] F. L. Litvin, J. Lu, D. P. Townsend and M. Howkins, "Computerized simulation of meshing of conventional helical involute gears and modification of geometry," Mechanism and Machine Theory, 34 (1999) 123-147.

[14] F. T. Litvin, I. Gonzalez-Perez, A. Fuentes, D. Vecchiato and T. M. Sep, "Generalized concept of meshing and contact of involte crosses helical gears and its application," Computer Methods in Applied Mechanics and Engineering, 194 (2005) 3710-3745.

[15] C. Weber and Banaschek, "Deformation and profile relief of spur-toothed and helical gear wheels," Vol. 11, Friedr. Vieweg & Sohn, Braunschweig/Wiesbaden (1953).